

Solar Electric Propulsion Subsystem Architecture for an All Electric Spacecraft

Dr. Michele Coletti, Dr. Angelo Grubisic,
Cheryl Collingwood and Prof. Stephen Gabriel
*University of Southampton,
United Kingdom*

1. Introduction

For many space missions, both a main propulsion subsystem and additional attitude control (AOCS) propulsion subsystem are required. These subsystems normally use different propellants, hence require separate tanks, different flow control units (FCU) and, in case of solar electric propulsion (SEP), separate power processing units (PPU). This leads to increases in total mass of the spacecraft and complexity while reducing system specific impulse.

One possibility to alleviate this problem would be to develop a main *and* an AOCS propulsion technology which could be integrated, sharing some of the components required for their operation, hence reducing system mass. A spacecraft employing such combined technologies as part of an SEP system is referred to as an “All-electric-spacecraft” (Wells et al., 2006).

In this chapter, the system design for an all-electric-spacecraft will be presented. A gridded ion engine (GIE) is proposed as a main propulsion subsystem with hollow cathode thrusters (HCT) considered for the AOCS propulsion subsystem. The mission considered during this study is the ESA European Student Moon Orbiter (ESMO), which the University of Southampton proposed to use SEP for both attitude control and main propulsion. During the ESMO phase-A study, a full design of the SEP subsystem was performed at QinetiQ as part of a wider study of the mission performed in conjunction with QinetiQ staff and funded by ESA. The output of this study will be here presented to explain the concept of the all-electric-spacecraft, its benefits, drawbacks and challenges.

1.1 The european student moon orbiter mission

ESMO is a student mission sponsored by the European Space Agency that started in 2006 and that, at present, is planned to be launched in early 2014 (http://www.esa.int/esaMI/Education/SEML0MPR4CF_0.html). ESMO will be completely designed, built and operated by students from across Europe resulting in the first European student built satellite reaching the moon. ESMO will be launched in a geostationary transfer orbit (GTO) as a secondary payload and from there will have to use its onboard propulsion to move to a lunar polar orbit. The payload will consist of a high resolution camera for optical imaging of the lunar surface.

3. SEP subsystem definition

As already anticipated in the introduction, the SEP subsystem proposed by Southampton University was based on the idea of an all-electric spacecraft, where a gridded ion engine provides primary propulsion and where hollow cathode thrusters are used to unload momentum from the reaction wheels. The gridded ion engine is based on the flight model hardware of the GOCE (Gravity and Ocean Open Circulation Explorer) mission T5 GIE, developed by QinetiQ (Edwards et al., 2004), whereas the HCTs to be used for AOCS will be based on the T5 discharge cathode.

The proposed SEP subsystem comprises:

- a single T5 GIE.
- eight HCTs used for AOCS functions.
- one or two (depending on the subsystem configuration) power processing units (PPU) to process and supply power to the T5 GIE and to the HCTs.
- one or two (depending on the subsystem configuration) flow control units (FCU) to regulate the propellant flow to the T5 GIE and to the HCTs.
- a tank for propellant storage.

During the course of this study, it has been assumed that the thruster to be used onboard ESMO will have the same performance as the GOCE T5 GIE (Table 1).

	GOCE T5
Thrust	1-20 mN
Specific Impulse	500-3500 s
Power	55-585 W

Table 1. T5 GOCE performance (Wells et al., 2006)

3.1 SEP subsystem design options and trade off

Three different design options were identified for the SEP subsystem, based on the level of integration between the GIE and HCTs.

Option 1 - High mass, low risk, low cost

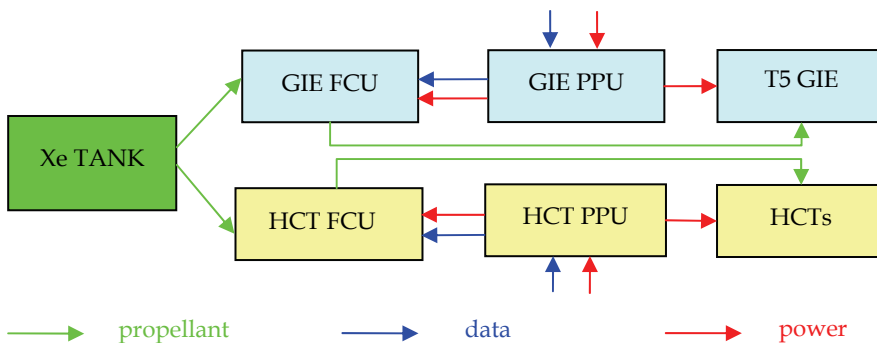


Fig. 1. First SEP subsystem architecture option: high mass, low risk, low cost

This is the option with the lowest risk and cost. Only the propellant tank is shared between the main propulsion and AOCS propulsion systems, hence leaving the more critical (and more expensive) components, such as the flow control units and the power processing units, unaltered. The low level of risk and cost is reflected in a low level of integration but results in a high system mass.

Option 2 – Medium mass, low risk, low cost

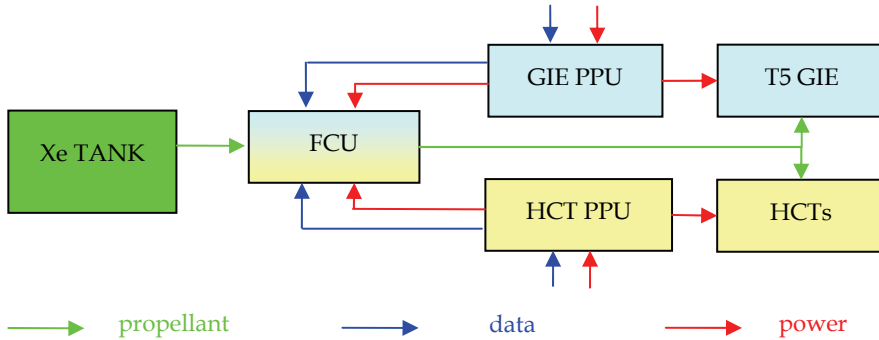


Fig. 2. Second SEP subsystem architecture option: medium mass, low risk, low cost

This option differs from the first by integrating the GIE and HCT flow control units into a single FCU. This provides a reduction of the system mass, whilst the cost and risk are kept relatively low since the PPUs (regarded as the most critical component) are left unmodified. Separate PPUs, able to supply the T5 GIE and the T5 HCTs already exist. An integrated PPU, able to supply both a GIE and several HCTs requires development and so will bring a high level of cost.

Option 3 – Low mass, high risk, high cost

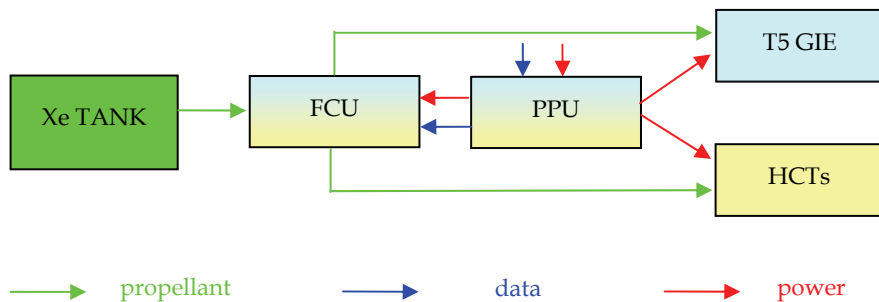


Fig. 3. SEP subsystem architecture option three: low mass, high risk, high cost

The level of integration is maximized in this final option, with the tank, PPU and FCU all being shared between the GIE and the HCTs. This leads to the lowest achievable system mass but conversely results in a high level of risk, since a new PPU must be designed able to supply both the GIE and several HCTs.

Considering that this study was carried out for a student mission with strict budget constraints, and that an EP mission to the Moon is in itself challenging, option 2 was

selected since it provides a low level of risk, whilst providing a medium level of integration and a relatively low system mass in comparison to the two non-integrated systems.

Once the general architecture has been fixed two other tradeoffs were carried out.

The first concerns compensation of the torque caused by any thrust misalignment of the main engine. Considering the long duration of the mission, associated with the long transfer time from GTO to the Moon for a SEP subsystem, the amount of propellant needed for the HCTs to compensate the torque is not negligible. Three options are available to reduce the thrust misalignment of the main engine; use of a gimbal, use of thrust vectoring or the choice to use additional propellant and accept the losses.

Thrust vectoring can be achieved using a set of movable grids on the GIE (Jameson, 2007). This technique is still experimental and hence, due to the level of risk involved, this solution was discarded. A gimbal is a relatively heavy, complex and expensive component whereas carrying additional propellant would be by far the simplest approach, though adversely affecting the overall mass budget.

The second trade-off to be carried out concerned the operation of the HCTs. Two possible options were identified: one option was to utilize a dedicated HCT PPU, able to drive as many HCTs as required whilst also driving the main propulsion system, the second option involved use of a switchbox utilizing the neutralizer cathode supply present inside the T5 GIE PPU.

Overall, four options exist for the subsystem design:

- HCTs driven by a dedicated PPU.
- HCTs driven by the neutralizer supply inside the T5 PPU via a switchbox.
- HCTs driven by a dedicated PPU plus a gimbal to reduce thrust misalignment.
- HCTs driven by the T5 PPU via a switchbox plus a gimbal to reduce thrust misalignment.

A comparison between all these options is reported in Table 2.

It is evident from Table 2 that the use of a gimbal produces a significant increase to the overall AOCS related mass. This option was therefore discarded.

The mass of the two remaining options differs by 4kg, due to the presence (or not) of a dedicated HCT PPU. These two options were traded against each other due to the cost and operational impact that the presence of a dedicated HCTs PPU would have.

The cost related to the development of a dedicated HCTs PPU would be substantial, based on estimates provided by QinetiQ; the cost would be twice that for development of a switchbox.

Regarding operation of the spacecraft, it must be noted that a switchbox offers no flexibility in the operation of the GIE and HCTs, since each time the HCTs must be used, the GIE must be switched off. Considering that the HCTs will be needed for a period from 1/3 to 1/6 of each orbit, the use of a switchbox would significantly reduce the average thrust produced by the GIE and consequently increase the transfer phase length and propellant required. The use of a dedicated PPU will instead allow both the main thruster and the HCTs to operate at the same time though, due to the limited power availability, the T5 GIE will have to be throttled down to free enough power for the HCT operations. More importantly, not having to switch off the main thruster each time the HCTs are used and perform a GIE shut-down and start-up procedure, management of the thruster subsystem is simplified.

Following the trade off studies, the use of a dedicated HCT PPU was chosen as the baseline option.

	Dedicated HCTs PPU without gimbal		Dedicated HCT PPU with gimbal		Switchbox without gimbal		Switchbox with gimbal	
	Mass	Margin	Mass	Margin	Mass	Margin	Mass	Margin
Thrust misalignment propellant mass	3 Kg	20%	0 Kg	20%	3 Kg	20%	0 Kg	20%
Solar pressure, safe manoeuvres and initial despin	1 Kg	20%	1 Kg	20%	1 Kg	20%	2 Kg	20%
HCT PPU	4 Kg	15%	4 Kg	15%				
gimbal			7 Kg	5%			7 Kg	5%
Switchbox					0.5 Kg	20%	0.5 Kg	20%
Total AOCS related mass	9.4 Kg		13 Kg		5.4 Kg		10.35 Kg	

Table 2. Comparison between a dedicated HCTs PPU and a switchbox with or without a gimbal

4. SEP baseline design description

The baseline design comprises:

- A single flight spare T5 GOCE GIT
- Eight HCTs (to provide some level of redundancy)
- A T5 PPU
- A HCT PPU
- A FCU able to supply both the HCTs and the T5 GIT
- A pressurized Xenon tank

4.1 T5 gridded ion thruster

The QinetiQ T5 Ion Thruster is a conventional electron bombardment, Kaufman-type GIE (a schematic of which is shown in Fig. 4).

In this kind of thruster a DC discharge is established between a hollow cathode (HC) and a cylindrical anode. The energetic electrons emitted from the HC collide with neutral propellant atoms injected upstream, resulting in ionization. The efficiency of the ionization is enhanced by the application of an axial magnetic field to constrain the electron motion. The ions produced are then extracted and accelerated by a system formed of two perforated disks (called grids), across which a potential difference of about 1.5 kV is applied. An external HC, referred to as the neutraliser, emits the electrons necessary to neutralise the space charge of the emerging ion beam.

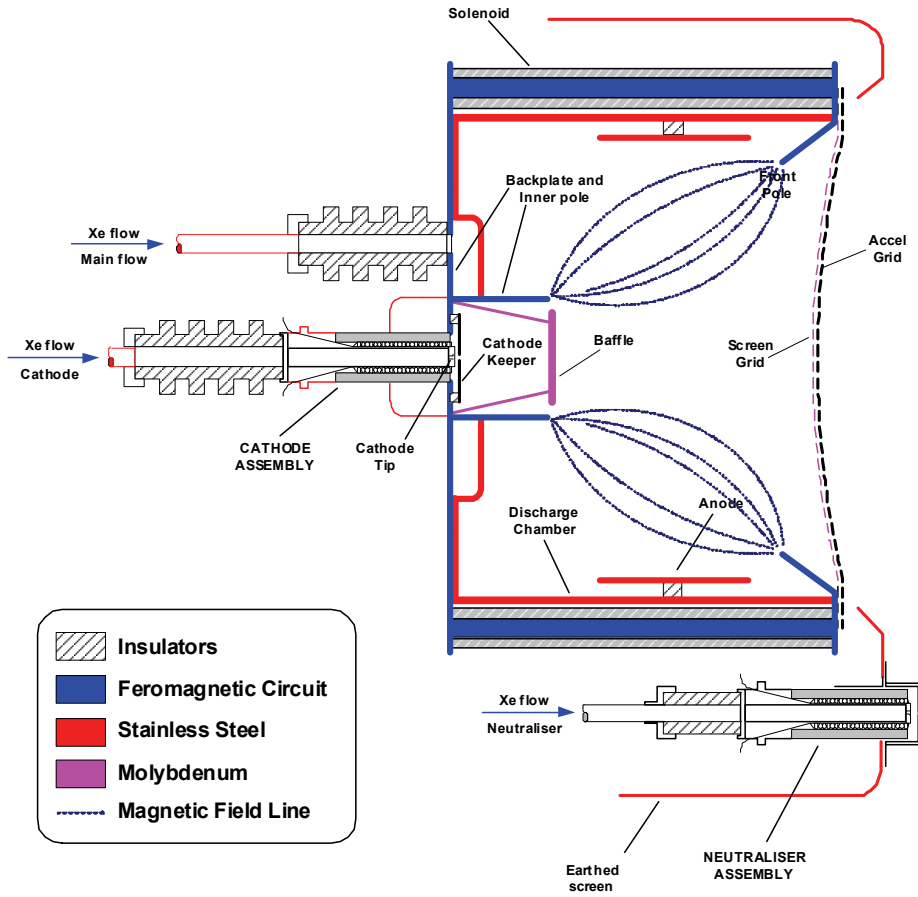


Fig. 4. A Kaufmann type gridded ion thruster schematic (T5) (image courtesy of QinetiQ)
 The T5 GIT specifications for the GOCE application are reported in Table 3

Mass	1.7 kg
Dimensions	Ø 170 mm x 200 mm long
Mean Power Consumption	up to 600 W @ 20mN
Thrust Range	1 to 20 mN
Specific Impulse	500 s to 3500 s (across thrust range)
Total Impulse	> 1.5 × 10 ⁶ Ns (under GOCE continuous throttling conditions)
T5 capability	> 8500 On/Off cycles

Table 3. T5 GIT specification (GOCE)

4.2 T5 Power processing unit

The power processing unit that will be used to drive the T5 GIE and the T5 FCU will be similar to the EADS Astrium Crisa GOCE PPU (Tato, de la Cruz, 2007). The PPU includes both a high voltage and a low voltage supply with the associated telemetry. The high voltage supply will be used to apply the required potential for the first of the two grids, whereas the low voltage supply will be used to operate the neutralizer and apply the potential for the second of the thruster grids. A schematic of the PPU is displayed in Fig. 5 whilst specifications are reported in Table 4.

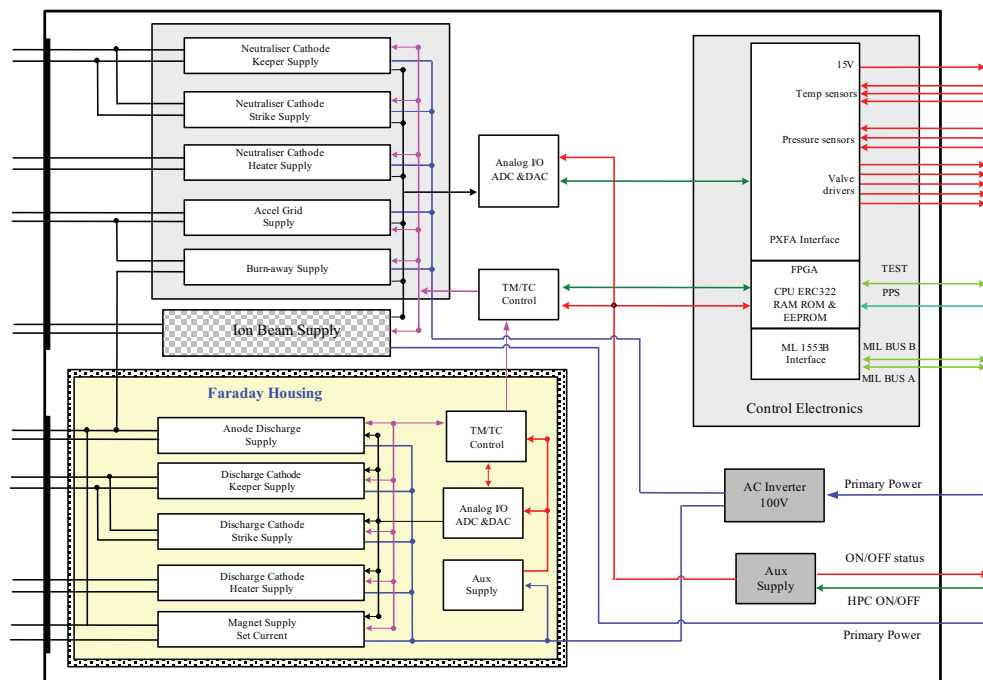


Fig. 5. GOCE PPU schematic (image courtesy of EADS Astrium Crisa)

Mass	16 kg
Dimensions	300 x 250 x 150 mm
Operating temperature	-20 °C to +50 °C
Operating lifetime	15 years in orbit (GOCE PPU qualification to mission duration of 2 years)
Nominal input voltage	22 - 37 V extended input range to 20 V without degradation
Maximum input current	37 A @ 22 V
Power	55-585 W
Electrical efficiency	Beam supply 92 - 95% other supplies ≥ 92%

Table 4. T5 GOCE PPU specification

4.3 Hollow cathode thruster

The thrust generated by a hollow cathode thruster in open-diode configuration (HC and a single anode) has been extensively characterized at the University of Southampton (Grubisic, 2009).

The basic feasibility of a HCT has been demonstrated and thrust levels up to several mN have been measured with specific impulse of the order of hundreds of seconds. More recently in light of its beneficial electrical characteristics, a T5 hollow cathode has undergone preliminary thrust characterization for application on ESMO. The experiment used a T5 STRV-A1 (Space Technology Research Vehicle) DRA (Defence Research Agency) flight-spares cathode launched in June 1994. This included an experiment to allow the hollow cathode assembly to demonstrate spacecraft electrostatic discharging. The cathode is rated at a maximum DC current of 3.2A at flow rates typically $0.04 - 1\text{mg}\cdot\text{s}^{-1}$ operating below 90W. The T5 cathode was originally designed for the main discharge cathode in the UK-10 ion engine and has been extensively characterized (Crofton, 1996). The cathode assembly contains a tungsten dispenser, 1.0mm ID \times 2.8mm OD \times 11mm, impregnated with a mixture of barium-oxide, calcium oxide and aluminates ($\text{BaO}:\text{CaO}:\text{Al}_2\text{O}_3$), which lowers the insert's work function for thermionic emission and maintains a working temperature of $\sim 1000^\circ\text{C}$. A solid tantalum tip welded to the cathode body contains an axial orifice 0.2mm in diameter and 1mm long. The face of the T5 cathode is shown in Fig.6.



Fig. 6. T5 Hollow Cathode Thruster

The open keeper has a 3mm diameter aperture and is mounted 3mm downstream of the cathode tip, with the whole assembly mounted on a UK-25 ion thruster back-plate. In typical hollow cathodes a keeper electrode usually draws approximately 1A of current, however in this study the cathode is operated in an open-diode configuration with the full discharge current being drawn to the keeper, which is now termed the anode. Previous studies on this type of hollow cathode have incorporated a much larger anode disk and a secondary discharge between the keeper and the anode and applied magnetic fields to simulate a Kaufman ion engine environment.

Open-diode configuration is more representative of a standalone microthruster configuration with no need for a coupled discharge. Results for the various current conditions are shown in Fig. 7.

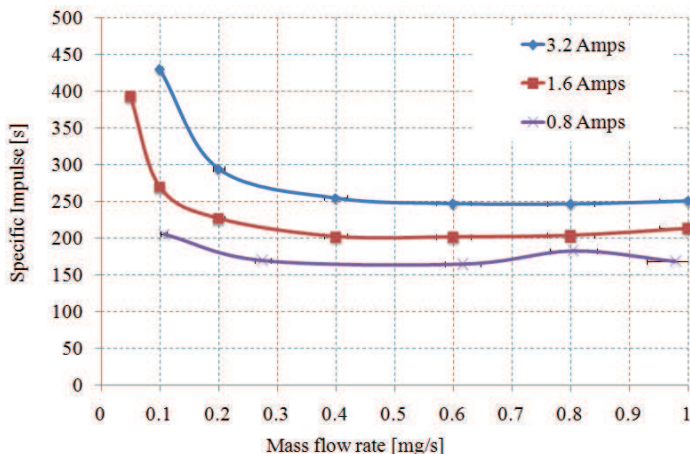


Fig. 7. Measurements of specific impulse with mass flowrate

Results show near monotonic dependence of specific impulse on discharge current with rapidly increasing performance below 0.4 mg/s^{-1} for the 3.2 and 1.6 Amp throttle settings with a less pronounced increase at 0.8 Amps. Since a change in flow rate results in a change in operating voltage it is seen that specific impulse can be correlated with specific power of the flow (J/mg) and a product of the discharge current and operating voltage, shown in Fig. 8. Operation at low powers ($<13\text{W}$) in the low current condition (0.8Amp) brings relatively high specific impulse of up to 165 seconds. At the high current condition operation at powers below 30W give specific impulse in the region of 250s. Further reduction in flow rate increases operating voltage and power invested in the flow. This results in a quadratic increase in specific impulse with declining thrust efficiency as convective and radiative losses begin to dominate.

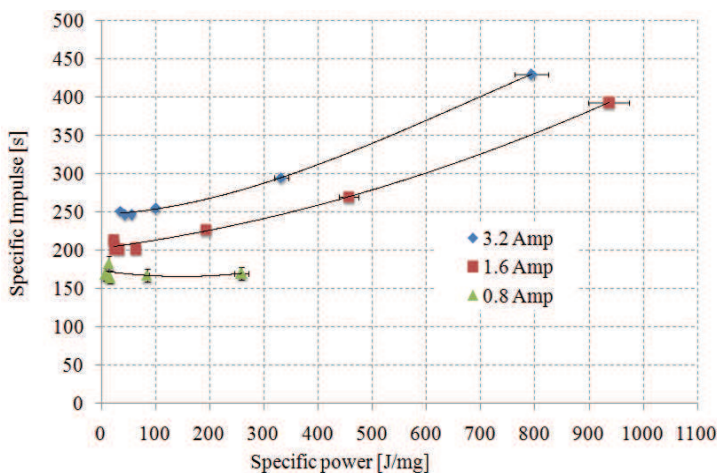


Fig. 8. Dependence of specific impulse on specific power at the various current levels with argon for the T5FO cathode

The highest specific impulse of 429s was attained at 3.2 Amps, with 1.1% thrust efficiency, 79W discharge power. Specific impulse can be traded for higher thrust to power ratios by increasing propellant flow rates or decreasing discharge current (however higher thrust efficiencies are obtained at higher discharge currents) generating thrust efficiencies of 14% ($200\mu\text{N/W}$) and specific impulse of 167s at 0.8Amps, and over 8% at the maximum rated current capacity of 3.2 Amps, with specific impulse $\sim 250\text{s}$ ($77\mu\text{N/W}$, 35W discharge power). Thrust production with respect to specific impulse is shown in Fig. 9. Up to 2.4mN could be generated at higher currents, with the maximum flow rate of 1mgs^{-1} with specific impulse over 250s.

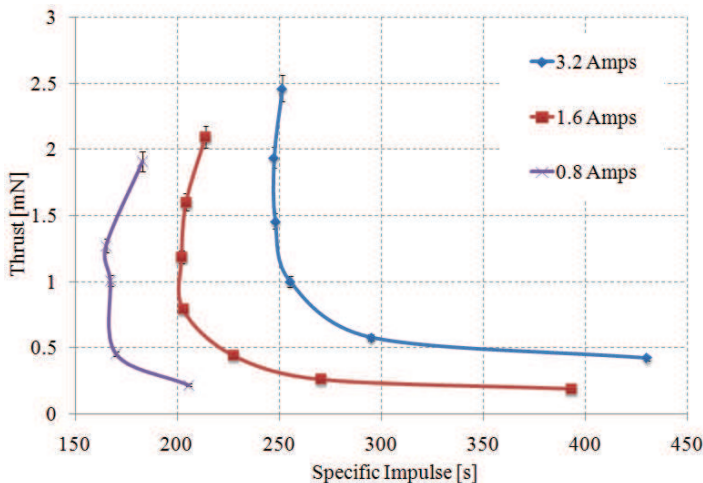


Fig. 9. Thrust and specific impulse attained at various current conditions in the T5 cathode

4.4 Hollow cathodes thruster PPU

The HCT PPU is sketched in 10.

The HCTs PPU consists of two anode and heater supplies and of a high voltage strike supply. The anode and heater supply is used to power the cathode heater during the start up phase and then, once the cathode is started using the HV strike supply, to power the cathode keeper to sustain its discharge. Two anode and heater supplies are present to allow the use of two HCTs at the same time that can be selected thanks to a system of switches. A mass estimate for this HCT PPU is 4 kg.

The anode and heater power supply is taken from the T6 neutralizer cathode PPU and is able to provide $3\text{A}@90\text{W}$. Such a supply is over-sized for a T5 hollow cathode (as can be seen from the data in Section 4.3) hence further study will be carried out to verify the possibility of powering two hollow cathodes in series (in this case with the PPU here presented we will be able to power four HCTs or alternatively we can use only one keeper heater supply saving mass).

4.5 Flow Control Unit

A suitable design for the FCU has been developed in collaboration with Thales Alenia Space (Matticari et al., 2005; Matticari et al., 2006; Van Put et al., 2004; van der List et al., 2006).

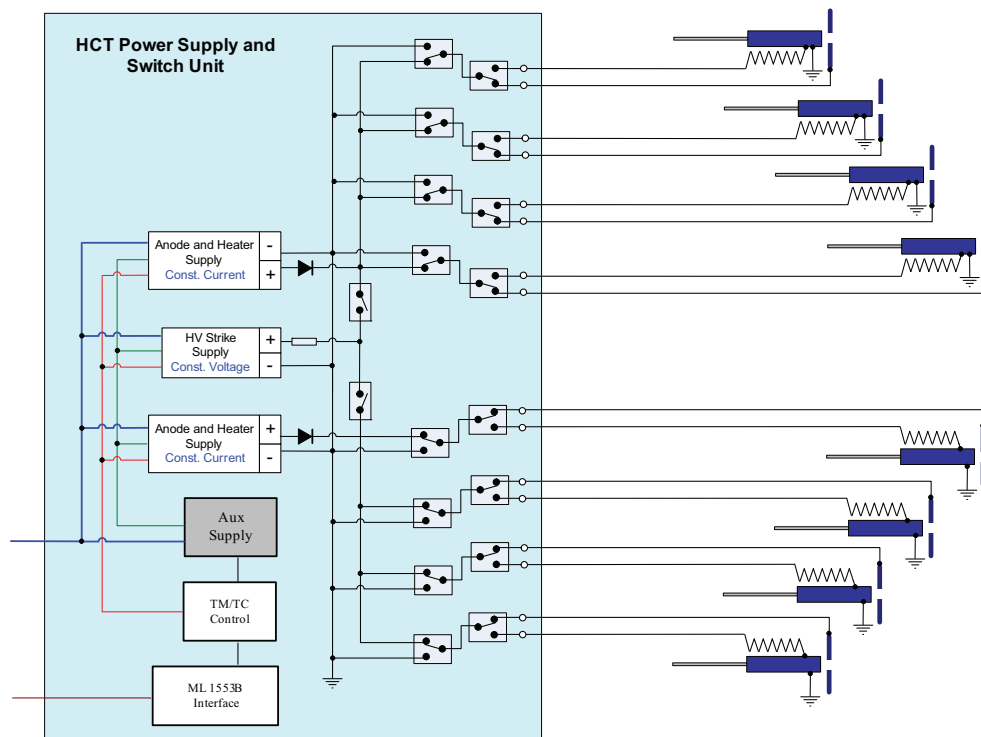


Fig. 10. HCT PPU schematic

Component	Mass flow rate [mg/s]	Pressure
T5 GIT	$0.07 - 0.53 \pm 0.007$	13 mbar (gas flow only) 20 mbar (gas flow & discharge)
T5 discharge cathode	0.1 ± 0.007	10 mbar (gas flow only) 100 mbar (gas flow & discharge)
T5 neutralizer	0.041 ± 0.006	10 mbar (gas flow only) 100 mbar (gas flow & discharge)
HCT	0.5 - 1.5	100 mbar ~ 1 bar (cold gas mode)

Table 5. Pressure and mass flow requirements

The design of the FCU, able to supply propellant to both the T5 GIE and to the HCTs, assumes that the HCTs will always be operated in pairs. Pressure and mass flow requirements are reported in Table 5.

The FCU is designed with a mass of 4 kg and a volume of approximately 300x200x100 mm. A schematic of the PPU is reported in 11.

The first element of the FCU is a gas purifier (F) needed to remove any impurities present in the Xenon gas supplied from the tank. After the filter, two high pressure solenoid valves (HPPV) used in closed loop with a low pressure transducer (LPT) and a mass flow sensor (MFS), regulate the pressure and mass flow rate to the value required for the HC. Two HPPV are used to provide redundancy in the high pressure branch of the FCU.

After MFS1 the flow is divided between the HCTs and the T5 thruster system. When the HCTs are off the flow is routed to the T5 thruster system. The HPPV is used to regulate the pressure required for the discharge/neutralizer HC and the T5 thruster according to system demands, hence there is no need to use LPPV1 and MFS2. LPPV2 and MFS3 are then used to fix the pressure and mass flow for the T5 GIT while LPC1 and LPC2 are used to regulate the mass flow rate to the neutralizer and discharge cathodes. If the HCTs are turned on, the relative on/off valves are opened. HPPV will be used to regulate pressure according to the HCT requirements and the mass flow rate according to the whole system's needs. LPPV1 and MFS2 will regulate the pressure and mass flow according to the T5 thruster system, hence LPPV2, MF3, LPC1 and LPC2 will work as if the HCTs are off. The LPCs will work such that the mass flow rates in two HCTs relative to the same axis are equal.

4.6 Propellant tank

The baseline propellant budget for the ESMO mission is shown in Table 6.

Propellant requirement	Xenon (Kg)	System margin	Xe with all margins
Transfer from GEO to low moon orbit	18.9 Kg	2%	19.8 Kg
Attitude control and initial despin	4 Kg	20%	4.8 Kg
Residuals		1.5%	0.4 Kg
Total mass			25 Kg

Table 6. Baseline ESMO propellant budget

The budget comprises the propellant processed by the T5 GIE needed for the transfer from GTO to lunar orbit, the propellant needed for the AOCS manoeuvres that is to be used by the HCTs and also any residual propellant that cannot be extracted from the tank (where 1.5% is a typical figure for this type of system). The propellant tank must be able to hold a minimum of 25 kg of Xenon. The Xenon storage pressure will be chosen from the Xenon isotherm curves reported in Fig 12. As it can be seen from Fig 12, the use of storage pressures higher than 100-150 bar does not produce any sensible reduction in volume, whilst it would produce a significant increase in mass, due to the higher pressure loads of the tank structure.

A 100 bar tank pressure was chosen as a baseline assuming room temperature (worst case); this results in 18 litres volume for 25 kg of Xenon whereas at 150 bar the tank volume is 15.3 litres. After performing a market search, a suitable tank was identified with the characteristics given in Table 7.

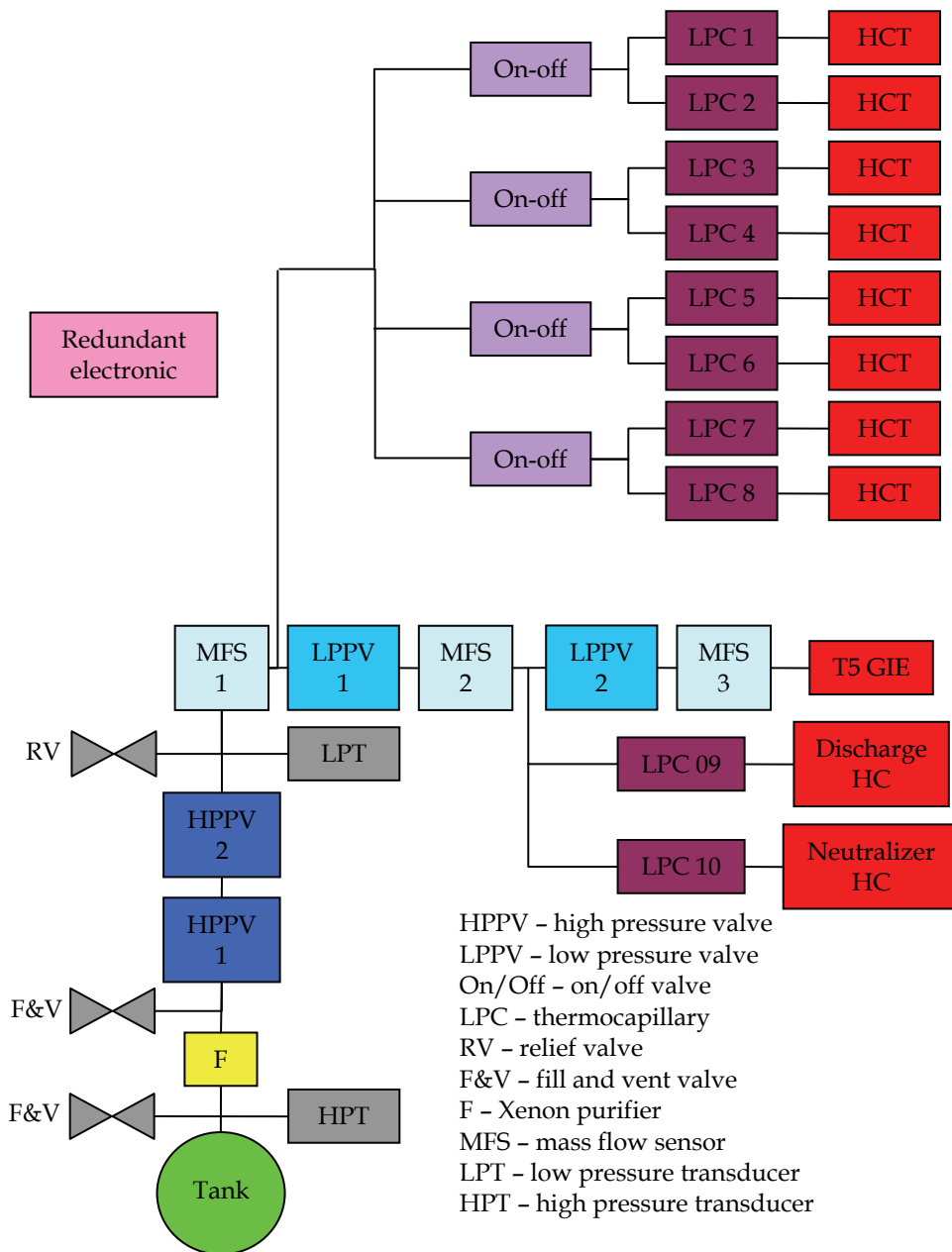


Fig. 11. Flow Controller Unit schematic

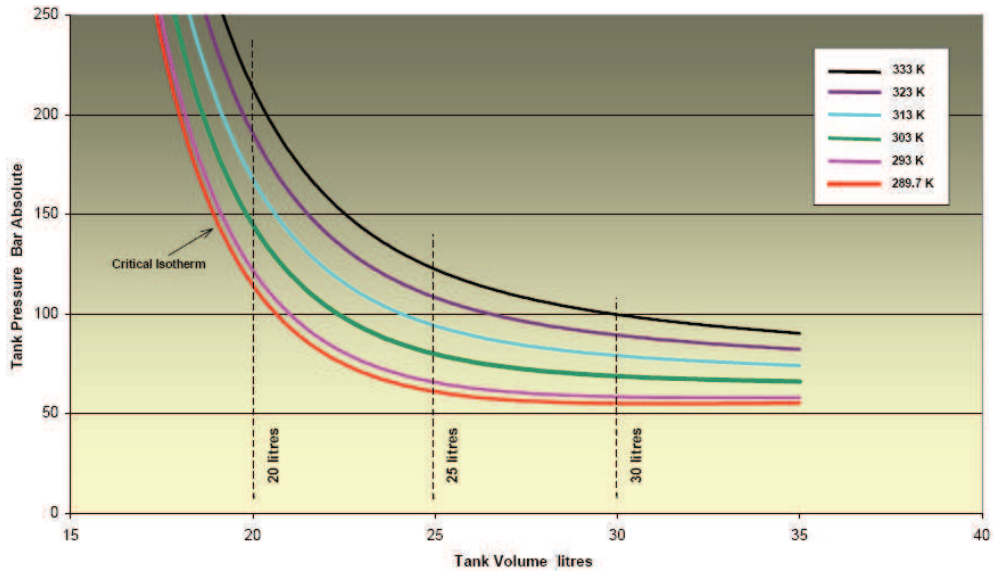


Fig. 12. Xenon isotherms for 30 Kg of Xenon

Shape	Cylindrical
Volume	19 litres
Mass	5 Kg
Maximum operating pressure (MEOP)	150 bar
Proof pressure	1.2 MEOP
Burst Pressure	1.5 MEOP
Material	Titanium T1000 liner with carbon fibre filament winding

Table 7. Thales Alenia Space Italia tank specifications

5. Conclusions

The full design of a solar electric propulsion subsystem for an all electric spacecraft has been presented which is applicable for the ESA ESMO mission.

The proposed propulsion subsystem is able to satisfy all mission requirements and achieves a medium level of integration between components providing non negligible mass savings. Table 9 displays a breakdown of the total subsystem mass.

Component	Mass
T5 GIT	1.7 Kg
GOCE-like PPU	16 Kg
FCU	4 Kg
8 x HCTs	0.8 Kg
HCT PPU	4 Kg
Tank	5 Kg
Propellant	31 Kg
Total Subsystem Mass	62.5 Kg

Table 8. ESMO Subsystem mass

The dry mass of the proposed SEP subsystem (31 kg) in this study can be compared to that of the SMART-1 electric propulsion subsystem of 29 kg (Kugelberg et al., 2004). The SMART-1 SEP subsystem comprises only a primary propulsion system, whereas the SEP subsystem in this study comprises both main and AOCS propulsion at a cost of only two extra kilograms.

6. Acknowledgments

The authors would like to thank Nigel Wells, Neil Wallace, Dave Mundy, Chris Dorn and Bill Levett from QinetiQ, Roger Walker from ESA (ESMO project manager) and Piero Siciliano and Mario Pessana from Thales Alenia Space for all their help and advice.

7. Appendix A. nomenclature

AOCS	=	attitude orbit and control subsystem
ESOC	=	European Space Operations Centre
F	=	Xenon purifier
FCU	=	flow control unit
F&V	=	fill and vent valve
GIT	=	gridded ion thruster
HCT	=	hollow cathode thruster
HPPV	=	high pressure valve
HPT	=	high pressure transducer
ID	=	internal diameter
LPC	=	thermocapillary
LPPV	=	low pressure valve
LPT	=	low pressure transducer
MFS	=	mass flow sensor
OD	=	outer diameter
On/Off	=	on/off valve
PPU	=	power processing unit
RV	=	relief valve
SEP	=	solar electric propulsion

8. References

- M. Crofton, "Evaluation of the United Kingdom Ion Thruster" J. Spacecraft and Rockets, Vol. 33, No. 5, 1996, pp. 739-747
- A. Grubisic, "Microthrusters Based on the T5 and T6 Hollow Cathodes", PhD Thesis, Aeronautics and Astronautics, University of Southampton, Southampton, 2009
- C. Tato and F. de la Cruz, "Power Control Unit for Ion Propulsion Assembly in GOCE Program," IEPC-2007-295, International Electric Propulsion Conference, Florence, Italy, September, 2007
- G. Matticari, G.E. Noci, P. Siciliano, G. Colangelo, R. Schmidt, "*Cold Gas Micro Propulsion Prototype for Very Fine Spacecraft Attitude/Position Control*", AIAA-2006-4872, 42nd AIAA/ASME/SAE/ASEE Joint Propulsion Conference and Exhibit, Sacramento, California, July 9-12, 2006
- G. Matticari, G.E. Noci, P. Siciliano, G. Martini, A. Rivetti, N. Kutufa, "*New Generation Propellant Flow Control Components: Status of Achievement at Alcatel Alenia Space Italia/Laben-Proel*", IEPC-2005-23, 29th International Electric Propulsion Conference, Princeton University, New Jersey, October 31 - November 4, 2005
- N. Wells, R. Walker, S. Green, A. Ball, "*SIMONE: Interplanetary Microsatellites for NEO Rendezvous Missions*", Acta Astronautica 59(8-11), 700-709, 2006.
- P. van Put, M. van der List, V. Yuce, "Development of an Advanced Proportional Xenon Feed Assembly for the GOCE Spacecraft", 4th International Spacecraft Propulsion Conference, Chia Laguna (Cagliari), Italy, 2-9 June, 2004.
- M. van der List, P. van Put, V. Yuce, J. Kuiper, "Next Generation Electrical Propulsion Feed Systems and Spin-off Micro-Propulsion Components ", ISU 2006 Conference, Strasbourg, France, 3-6 August 2006.
- N. Wells, R. Walker, S. Green, A. Ball, SIMONE: interplanetarymicrosatellites for NEO rendezvous missions, Acta Astronautica, 59 (8-11) (2006) 700-709.



Advances in Spacecraft Technologies

Edited by Dr Jason Hall

ISBN 978-953-307-551-8

Hard cover, 596 pages

Publisher InTech

Published online 14, February, 2011

Published in print edition February, 2011

The development and launch of the first artificial satellite Sputnik more than five decades ago propelled both the scientific and engineering communities to new heights as they worked together to develop novel solutions to the challenges of spacecraft system design. This symbiotic relationship has brought significant technological advances that have enabled the design of systems that can withstand the rigors of space while providing valuable space-based services. With its 26 chapters divided into three sections, this book brings together critical contributions from renowned international researchers to provide an outstanding survey of recent advances in spacecraft technologies. The first section includes nine chapters that focus on innovative hardware technologies while the next section is comprised of seven chapters that center on cutting-edge state estimation techniques. The final section contains eleven chapters that present a series of novel control methods for spacecraft orbit and attitude control.

How to reference

In order to correctly reference this scholarly work, feel free to copy and paste the following:

Michele Coletti, Angelo Grubisic, Cheryl Collingwood and Stephen Gabriel (2011). Electric Propulsion Subsystem Architecture for an All-Electric Spacecraft, *Advances in Spacecraft Technologies*, Dr Jason Hall (Ed.), ISBN: 978-953-307-551-8, InTech, Available from: <http://www.intechopen.com/books/advances-in-spacecraft-technologies/electric-propulsion-subsystem-architecture-for-an-all-electric-spacecraft>

INTECH

open science | open minds

InTech Europe

University Campus STeP Ri
Slavka Krautzeka 83/A
51000 Rijeka, Croatia
Phone: +385 (51) 770 447
Fax: +385 (51) 686 166
www.intechopen.com

InTech China

Unit 405, Office Block, Hotel Equatorial Shanghai
No.65, Yan An Road (West), Shanghai, 200040, China
中国上海市延安西路65号上海国际贵都大饭店办公楼405单元
Phone: +86-21-62489820
Fax: +86-21-62489821

© 2011 The Author(s). Licensee IntechOpen. This chapter is distributed under the terms of the [Creative Commons Attribution-NonCommercial-ShareAlike-3.0 License](#), which permits use, distribution and reproduction for non-commercial purposes, provided the original is properly cited and derivative works building on this content are distributed under the same license.